WORMGEAR GEOMETRY ADOPTED FOR IMPLEMENTING HYDROSTATIC LUBRICATION AND FORMULATION OF THE LUBRICATION PROBLEM

by

D.C. Sun and Qin Yuan

Department of Mechanical Engineering
State University of New York at Binghamton
Binghamton, New York 13902-6000

SEPTEMBER 1994

TABLE OF CONTENTS

Abstract

The geometrical parameters for a wormgear intended to be used as the transmission in advanced helicopters are finalized. The resulting contact pattern of the meshing tooth surfaces is suitable for the implementation of hydrostatic lubrication. Fluid film lubrication of the contact is formulated considering external pressurization as well as hydrodynamic wedge and squeeze actions. The lubrication analysis is aimed at obtaining the oil supply pressure needed to separate the worm and gear surfaces by a prescribed minimum film thickness. The procedure of solving the mathematical problem is outlined.

Nomenclature

(Most wormgear terminologies are listed in Table 1)

a	speed of sound
A	cross sectional area of the capillary flow restrictor
$A^{(km)}$	coordinate transformation matrix from S_m to S_k (See Report 1.)
B	isothermal bulk modulus
c_p	specific heat at constant pressure
c_v	specific heat at constant volume
D	hydraulic diameter, = $4A/s$
f_M	Moody friction factor
$\bar{f}_M$	mean Moody friction factor
g	clearance between meshing worm and gear surfaces
h	fluid film thickness
h_{min}	minimum film thickness
$[h_{min}]$	prescribed minimum film thickness
k	ratio of specific heats, = c_p/c_v
L	length of the capillary flow restrictor
m	mass flow rate
M	Mach number
p	fluid film pressure
P	reduced pressure
R_e	Reynolds number
s	wetted perimeter of A
S_j (x_j, y_j, z_j)	stationary worm coordinate system (See Report 1.)
S_n (x_n, y_n, z_n)	stationary gear coordinate system (See Report 1.)
S_1 (x_1, y_1, z_1)	moving worm coordinate system (See Report 1.)
S_2 (x_2, y_2, z_2)	moving gear coordinate system (See Report 1.)
S_3 (x_3, y_3, z_3)	moving gear coordinate system for clearance calculation

(u,v,w)	velocity components of fluid film flow in the (ξ,η,ζ) directions
(U,V)	velocity components of the worm surface relative to the gear surface, lying in the tangent plane of the worm surface and essentially in the ξ and η directions
v	mean flow velocity in the flow restrictor
W	load carrying capacity of the fluid film
x	coordinate axis along the flow restrictor
α_n	normal pressure angle of the wormgear
β	apex angle of the generating plane
θ_2	gear rotation angle (See Report 1.)
μ	viscosity
(ξ,η,ζ)	coordinate system for lubrication analysis
ρ	density
ψ_2	worm rotation angle (See Report 1.)

Subscripts

$( )_a$	at the ambient condition
$( )_r$	at the end of the recess
$( )_s$	at the end of the supply chamber
$( )_1$	in recess 1*
$( )_2$	in recess 2*

---

* As wormgear nomenclature, $( )_1$ and $( )_W$ refer to the worm; $( )_2$ and $( )_G$ refer to the gear.

1 Background and Objectives of the Study

The ongoing project (NASA Research Grant NAG3-1316) studies the feasibility of using a hydrostatically lubricated wormgear as the transmission in advanced helicopters. The selection of a wormgear type suitable for the intended application was made, and a computer program was developed capable of evaluating the kinematic and load sharing properties of the selected wormgear for any combinations of gear parameters and dimensions. The work was reported in Sun and Yuan (1994a, hereafter to be referred to as Report 1). The results in this report were computed for gear dimensions that basically followed the gear standards. Later it was deemed worthwhile to investigate the possibility of using a non-standard tooth profile where the pressure angle is different on the two sides of the tooth, for the purpose of more efficiently producing the needed output torque. A detailed study of the relative merits between the symmetric and non-symmetric tooth profiles was conducted and was reported in Sun and Yuan (1994b, hereafter to be referred to as Report 2). These investigations paved the way for the final adoption of an optimal wormgear geometry and for further lubrication studies.

The present report describes the subsequent developments: A set of wormgear parameters was selected in such a way that the contact pattern of the meshing tooth surfaces was suitable for the implementation of hydrostatic lubrication. After the fluid film load bearing regions on a gear tooth were determined, the oil supply configuration on the tooth surface was designed. Fluid film lubrication of the contact was formulated considering external pressurization as well as hydrodynamic wedge and squeeze actions. The flow in the flow restrictors was analyzed which linked the needed oil supply pressure with the recess pressures, which in turn are linked with a prescribed minimum oil film thickness. The report then outlines the procedure of solving the mathematical problem.

2 Wormgear Geometry

2.1 Finalized Geometrical Parameters and Contact Features

The procedure of selecting wormgear dimensions typically starts with a known speed ratio and a known center distance. In the intended application the power output of each worm is 4000 kW, the speed ratio is 110, the gear rotation speed is 130 r/min, and the diameter of the gear is about 1500 mm (Chaiko, 1990). Based on these requirements and by following closely the gear standards (AGMA, 1965; Dudley, 1984), a set of gear dimensions were laid out in Report 1. In particular, the normal pressure angle was the standard 20 deg and the tooth profile was symmetric. This choice was shown in Report 2 to be superior than the alternative non-symmetric profile. This is mainly because the symmetric profile allows a longer face width of the worm, hence a greater number of meshing teeth to share the load.

Report 2 also shows that the apex angle β has a profound influence on the distribution of contact lines. When β is small, the contact lines crowd around the mid-plane; as β increases, the contact lines spread and cover more of the tooth flank. Traditionally a uniform distribution of contact lines on the tooth flank is considered to be better because wear of the tooth surface would be more even. But for the wormgear under investigation, which is enhanced by hydrostatic lubrication, pressurized oil must be brought to the contact and it is convenient to fix the oil supply configuration on the gear tooth surface. Then, it is imperative to confine the contact lines to a target area of the tooth flank. After careful adjustment of the apex angle and comparison of results, the final choice of $\beta = 3$ deg was made. The finalized wormgear dimensions and parameters are summarized in Table 1.

Figure 1 shows a typical wormgear position where a certain tooth, denoted as tooth No. 0, is at $\theta_2 = 0$. It can be seen that at this position

ten pairs of teeth are in meshing, beginning from tooth No. 2 and ending with tooth No. 11. The contact lines on several of these teeth are shown in Figs. 2. In these figures the unit of the coordinates is millimeter and the gear tooth domain (shown in its true proportion) is marked by solid lines. For the gear surface coordinate system $S_2(x_2,y_2,z_2)$, refer to Fig. 3.1 of Report 1. Several contact features can be identified: (1) On the majority of the teeth there are two contact lines, located more or less symmetrically on the two sides of the mid-plane. This means that potentially there are two fluid film load bearing regions on the tooth flank. (2) The contact lines run across the tooth flank more or less in parallel with the mid-plane. This means that the contact lines are nearly perpendicular to the velocity of the worm surface, which is advantageous for generating the hydrodynamic wedge action. (3) In contrast to the case of β = 5 deg, which is shown in Figs. 3.7 of Report 1, the contact lines now lie much closer to the mid-plane. This means that contact is confined to a small area surrounding the mid-plane, which is convenient for designing the oil supply configuration.

2.2 Clearance Between the Meshing Surfaces

Because the positions of contact lines vary as the wormgear rotates, the clearance between the meshing surfaces is a complicated function both of the position on the tooth flank and of time. The tedious procedure of computing the clearance function is briefly described in Appendix 1.

Some representative results on the clearance shape are given below for illustration. Figures 3 show the clearance profile, for several meshing teeth, in a (y_2,z_2) plane whose x_2 location is on the pitch circle. In the figures * denotes a point on the worm surface and O denotes a point on the gear surface. It is seen that, at the beginning when the worm and gear run into meshing, there are two contact points along the profile and the clearance is small between the two contact points; then toward the end of the meshing

zone one contact point disappears and the clearance becomes large.

2.3 Relative Velocities between the Meshing Surfaces

The velocity of the worm surface relative to the gear surface at a contact point is given by Eqs. 38 of Report 1. For lubrication analysis the relative velocity at a general point in the fluid film regions is needed, which can be obtained by first knowing the coordinates of the corresponding points on the worm and gear surfaces, then finding the velocities of these points. For the latter quantities, note that the velocity of a point on the worm (gear) surface is simply the distance from this point to the worm (gear) axis multiplied by the worm (gear) rotation speed. While the computation is laborious, a general feature may be transparent: Because the fluid film regions are chosen to be close to the mid-plane and the speed ratio is large, the relative velocities in these regions are nearly perpendicular to the mid-plane. Some details of computing the relative velocities are given in Appendix 2.

2.4 Normal Force on a Gear Tooth

The normal force on a gear tooth is the load the fluid film must withstand. This information is needed in the lubrication analysis. The distribution of load among meshing teeth was analyzed in Report 1 based on a load sharing hypothesis. Applying the analysis to the wormgear geometry presently chosen, the normal force on a gear tooth and the torque variation along the worm coil are obtained. To evaluate the effect of friction a Coulomb friction coefficient of 0.07, a typical value when fluid film lubrication is not established at the contact, is used in the computation. The results are shown in Figs. 4 and 5. In these figures, * represents the case with friction and O represents the case without friction.

Figure 4 shows the variation of the normal force on a gear tooth as the latter moves through the meshing zone (using the gear rotation angle θ_2 as a time parameter). The difference between including and not including friction cannot be detected. This means that, for the specified power output, the lubricant film must withstand almost the same load whether friction is present or not. Note that the peak normal force is higher than in the case of $\beta = 5$ deg, which is shown in Fig. 4.4 of Report 1. This is because in the present case the second enveloping contact line disappears earlier in the meshing zone. Compare Figs. 2 with Figs. 3.7 of Report 1. As a result, the total length of contact lines (at any instant) is shorter, then by the load sharing hypothesis, the unit load level becomes higher. This is a price paid for having the contact lines lie closer to the mid-plane.

Figure 5 shows the torque variation along the worm coil. By comparing with Fig. 34 of Report 2, one can see that the torque level in this case is also slightly higher than in the case of $\beta = 5$ deg. Note also that the presence of friction causes a much higher torque level. This is because the direction of friction is very close to that of the tangential force on the worm. Hence, a large part of the input torque must be spent to overcome the friction torque. With fluid film lubrication established at the contact, the friction coefficient would be reduced to the order of 10^{-3}. Then, the input worm torque needed to produce the specified output power would be greatly reduced.

3 Formulation of the Lubrication Problem

3.1 Oil Supply Configuration

The results of Section 2.1 show that the contact between the worm and gear surfaces is confined to a small area surrounding the mid-plane. This area consists of two regions covered respectively by the first and second

enveloping contact lines and extends approximately 25 mm in each direction from the mid-plane. This area, boxed by dashed lines in Fig. 6, is chosen for the application of fluid film lubrication. Taking advantage of the existence of two load bearing regions, the oil supply configuration is chosen to consist of two oil grooves which run parallel to the mid-plane and are symmetrically placed on the two sides of the mid-plane. Oil is brought to the grooves through capillary flow restrictors which are connected to a single oil supply chamber. The dimensions of the grooves and their distance from the mid-plane are adjustable design parameters. In computing the fluid film pressure the actual boundary of the lubrication region is located where the fluid film thickness reaches a large value (e.g. 0.1 mm). Thus, the lubrication region is not exactly the boxed region shown in Fig. 6.

3.2 Analysis of Fluid Film Pressure

Pressure in the fluid film is generated by three mechanisms: One is the supply of pressurized oil to the contact area through the oil grooves, which is called the hydrostatic action. The second is the sliding motion of the worm surface (relative to the gear surface) that drags oil into the small clearance of the contact area, which is called the hydrodynamic wedge action. There is still the third, viz. the normal approach of the worm surface to the gear surface, which is called the squeeze action. The squeeze action is present when the clearance varies with time. The equation governing the pressure (the Reynolds equation) can be obtained by analyzing the fluid film flow using the lubrication theory (Sun, 1991), then the pressure is obtained by solving the Reynolds equation along with appropriate boundary and initial conditions.

The lubrication model may be constructed as follows: Consider one gear tooth surface as stationary and over which the worm coil surface moves. For convenience the gear surface is treated as flat, lying in the coordinate plane

(ξ,η) which coincides with the original generating plane (Section 3.3, Report 1). The fluid film thickness h is the sum of a prescribed minimum film thickness $[h_{min}]$ (considered known) and the clearance g between the meshing surfaces measured in the ζ direction which is normal to the (ξ,η) plane. The relation between the coordinate system (ξ,η,ζ) for the lubrication analysis and the coordinate system $S_2(x_2,y_2,z_2)$ are shown in Fig. 7. Note that the η axis is parallel to the x_2 axis. The velocity of the worm surface (relative to the gear surface) at any point in the fluid film regions, which is obtained in Section 2.3, is broken up into three components: $U(\xi,\eta,t)$ and $V(\xi,\eta,t)$ lying in the tangent plane of the worm surface and essentially in the ξ and η directions; and $\partial h/\partial t$ normal to the (ξ,η) plane. During the meshing period the load acting on the fluid film is given in Section 2.4. A schematic diagram of the lubrication model is shown in Fig. 8.

The fluid film flow is assumed to be isothermal. Since high supply pressure is anticipated, the effect of oil compressibility is considered. The density and pressure of oil are assumed to obey the relation:

$$\rho=\rho_a e^{\frac{p-p_a}{B}} \tag{1}$$

where p is the pressure, ρ the density, B the isothermal bulk modulus (considered to be a constant), and $(\ )_a$ denotes the ambient condition.

Within the lubrication approximations, the velocity components (u,v,w) of the fluid film obey the following simplified equations:

<u>The continuity equation</u>

$$\frac{\partial\rho}{\partial t}+\frac{\partial}{\partial\xi}(\rho u)+\frac{\partial}{\partial\eta}(\rho v)+\frac{\partial}{\partial\zeta}(\rho w)=0 \tag{2}$$

The (ξ,η,ζ) momentum equations

$$\frac{\partial p}{\partial \xi}=\mu\frac{\partial^2 u}{\partial \zeta^2}$$

$$\frac{\partial p}{\partial \eta}=\mu\frac{\partial^2 v}{\partial \zeta^2} \qquad (3)$$

$$\frac{\partial p}{\partial \zeta}=0$$

and the velocity boundary conditions:

$$\begin{aligned} &At \quad \zeta=0, \quad u=v=w=0 \\ &At \quad \zeta=h, \quad u=U(\xi,\eta,t) \\ &\qquad\qquad v=V(\xi,\eta,t) \\ &\qquad\qquad w=\frac{\partial h}{\partial t}+U\frac{\partial h}{\partial \xi}+V\frac{\partial h}{\partial \eta} \end{aligned} \qquad (4)$$

where μ is the viscosity of oil (considered to be a constant).

From the ζ momentum equation it can be seen that p is only a function of (ξ,η,t). Hence the ξ and η momentum equations can readily be integrated with respect to ζ. Using the velocity boundary conditions, one obtains:

$$\begin{aligned} u&=-\frac{\partial p}{\partial \xi}\frac{\zeta(h-\zeta)}{2\mu}+U\frac{\zeta}{h} \\ v&=-\frac{\partial p}{\partial \eta}\frac{\zeta(h-\zeta)}{2\mu}+V\frac{\zeta}{h} \end{aligned} \qquad (5)$$

By substituting u and v into the continuity equation, then integrating the equation from ζ=0 to ζ=h, and using the boundary conditions for w, one obtains the Reynolds equation:

$$\frac{\partial}{\partial \xi}\left(h^3 \frac{\partial P}{\partial \xi}\right) + \frac{\partial}{\partial \eta}\left(h^3 \frac{\partial P}{\partial \eta}\right) = \frac{6\mu}{B}\left[\frac{\partial}{\partial \xi}(PUh) + \frac{\partial}{\partial \eta}(PVh)\right] + \frac{12\mu}{B}\frac{\partial}{\partial t}(Ph) \tag{6}$$

where $P = e^{(p-p_a)/B}$ is a "reduced" pressure. In the equation the terms enclosed in square brackets on the right hand side are the wedge action terms; the term on the right hand side involving the time derivative is the squeeze term; the sliding velocity components (U,V) and the clearance function $h(\xi,\eta,t)$ are known functions; and P is the unknown. Note that using the reduced pressure as the unknown renders the Reynolds equation linear.

The boundary conditions for pressure are that the ambient pressure is prescribed at the boundary of the lubrication region, which is located where the fluid film thickness reaches a large value; and constant recess pressures, p_{r1} and p_{r2}, prevailing respectively in the two oil grooves. Initially the pressure in the lubrication region is the ambient pressure.

The pressure in the fluid film is to be solved from Eq. 6 and the above boundary and initial conditions. The pressure so obtained, when integrated over the fluid film regions, is required to balance the normal force acting on the gear tooth, as given in Section 2.4. The two recess pressures are related to a single oil supply pressure, p_s, prevailing in the supply chamber. Since the normal force is given as a function of time, the supply pressure thus determined is a function of time.

3.3 Flow Restrictor Analysis

Flow passage must be provided between the oil supply chamber and the oil recess. This flow passage is called the flow restrictor. A schematic arrangement of the flow restrictor in a hydrostatic bearing is shown in Fig. 9. Flow restrictor analysis is an integral part of the theory of hydrostatic lubrication. There are two common types of flow restrictors: orifice and

capillary. Flow in the former is typically treated as an incompressible inviscid flow; and in the latter as an incompressible viscous flow. In the case under investigation, there are two oil recesses, i.e. the two oil grooves, hence there need to be two flow restrictors. It is convenient to use capillary flow restrictors because the supply oil must go through the gear body to reach the oil grooves. Besides, since high supply pressure is anticipated, the effect of oil compressibility is included in the flow restrictor analysis.

Compressible flow of a liquid through a capillary may be treated as a Fanno-line type flow, in which the needed friction factor may be obtained from the Moody diagram. The Fanno-line flow of a gas is described in a treatise on gasdynamics (Liepmann and Roshko, 1957). The Moody diagram, along with its various empirical correlation formulas, can be found in a standard fluid mechanics textbook (Fox and McDonald, 1992). The analysis proceeds as follows:

Consider a one-dimensional quasi-steady isothermal compressible flow with negligible body force in a tube of constant cross sectional area A. Let the streamwise coordinate be x. The continuity equation reads:

$$\frac{d}{dx}(\rho v) = 0 \tag{7}$$

The momentum equation reads:

$$\rho v \frac{dv}{dx} = -\frac{dp}{dx} - \frac{f_M}{D}\frac{\rho v^2}{2} \tag{8}$$

where f_M is the Moody friction factor and D the hydraulic diameter (D=4A/s, s being the wetted perimeter of the tube's cross section). In addition, Eq. 1 provides the relation between p and ρ. Thus, there are three equations to solve for the three unknowns p, ρ, and v.

To facilitate solution of the system, the Mach number is introduced:

$$M = \frac{v}{a} \tag{9}$$

where a is the speed of sound which may be expressed in terms of the isothermal bulk modulus of the liquid by means of thermodynamics (Moran and Shapiro, 1992):

$$a^2 = \left(\frac{\partial p}{\partial \rho}\right)_{isentropic} = k\left(\frac{\partial p}{\partial \rho}\right)_{isothermal} = \frac{kB}{\rho}, \qquad \text{where } k = \frac{c_p}{c_v} \tag{10}$$

Writing Eqs. 7-9 and Eq. 1 in differential forms, one obtains:

$$\frac{d\rho}{\rho} + \frac{dv}{v} = 0 \tag{11}$$

$$2\frac{dv}{v} = -\left(\frac{2}{kM^2}\right)\frac{dp}{B} - \frac{f_M dx}{D} \tag{12}$$

$$2\frac{dM}{M} = \frac{d\rho}{\rho} + 2\frac{dv}{v} \tag{13}$$

$$\frac{d\rho}{\rho} = \frac{dp}{B} \tag{14}$$

These four equations can be solved algebraically for the four quantities $d\rho/\rho$, dp/B, dv/v, and dM/M. The result is that the first three differentials are all expressed in terms of dM/M while the latter is uncoupled from the rest in a single equation. Thus:

$$\frac{d\rho}{\rho} = -2\frac{dM}{M}$$

$$\frac{dp}{B} = -2\frac{dM}{M}$$

$$\frac{dv}{v} = 2\frac{dM}{M} \qquad (15)$$

$$\left(\frac{1}{kM^2} - 1\right)\frac{dM}{M} = \frac{f_M dx}{4D}$$

These expressions can then be integrated from the inlet to the exit of the tube to yield:

$$\rho_s M_s^2 = \rho_r M_r^2$$

$$\frac{v_s}{M_s^2} = \frac{v_r}{M_r^2}$$

$$\frac{p_s}{B} + \ln M_s^2 = \frac{p_r}{B} + \ln M_r^2 \qquad (16)$$

$$\left(\ln M_s + \frac{1}{2k}\frac{1}{M_s^2}\right) - \frac{\overline{f_M} L}{4D} = \ln M_r + \frac{1}{2k}\frac{1}{M_r^2}$$

where L is the length of the tube, $\overline{f_M}$ the mean friction factor, $(\ )_s$ and $(\ )_r$ denote respectively the inlet (at the supply chamber end) and the exit (at the oil recess end) conditions.

For a smooth tube the Moody friction factor is only a function of the Reynolds number which is defined as:

$$R_e = \frac{\rho v D}{\mu} = \frac{4\dot{m}}{\mu S} \qquad (17)$$

where $\dot{m}=\rho vA$ is the mass flow rate. Empirical correlation formulas for the Moody friction factor may be given as follows:

$$For\ R_e<2300,\quad \overline{f_M} = \frac{64}{R_e}$$

$$For\ 2300<R_e<10^5,\quad \overline{f_M} = \frac{0.3164}{R_e^{0.25}} \tag{18}$$

$$For\ R_e>10^5,\quad \overline{f_M} = 0.25\left(\log_{10}\frac{5.74}{R_e^{0.9}}\right)^{-2}$$

Equations 16 essentially provide a relation between p_r and p_s. The relation becomes lucid by observing the following: Suppose p_r is known. From p_r and the pressure field surrounding the oil groove, the mass flow rate from the groove into the fluid film region can be determined. This mass flow rate must also be the $\dot{m}$ through the flow restrictor. From p_r one knows ρ_r and a_r; from $\dot{m}$ one further knows v_r, M_r, and R_e. Knowing R_e, one can calculate $\overline{f_M}$ from Eqs. 18. Then, M_s can be determined from the last equation, and p_s from the third equation, of Eqs. 16.

3.4 Solution Procedure

The lubrication analysis is aimed at obtaining the oil supply pressure needed to separate the worm and gear surfaces by a prescribed minimum oil film thickness. The analysis consists of two coupled parts as described in Sections 3.2 and 3.3. The mathematical problem has to be solved numerically and by iteration. The quantities to be iterated are the two recess pressures, p_{r1} and p_{r2}, prevailing respectively in the two oil grooves. The solution procedure may be as follows:

(1) Choose a gear position or time, θ^*.

(2) Assume p_{r1} and p_{r2}; and solve the unsteady Reynolds equation for p.

(3) Compute the load carrying capacity W by integrating the pressure over the fluid film regions; and the mass flow rates $\dot{m}_1$ and $\dot{m}_2$ through the two flow restrictors.

(4) Compute p_{s1} from p_{r1} and $\dot{m}_1$; likewise compute p_{s2} from p_{r2} and $\dot{m}_2$.

(5) If p_{s1} equals p_{s2} and W equals the normal force acting on the gear tooth at this time, the solution has been found. Go to (1) for the next time step. Otherwise go to (2) and revise p_{r1} and p_{r2}.

The procedure is outlined by a flow diagram in Fig. 10.

Note that the supply pressure so obtained are for the prescribed $[h_{min}]$. In the beginning and toward the end of the meshing period the normal force may be small enough that hydrodynamic lubrication alone is adequate. Hence a pre-procedure is added to the above procedure. The pre-procedure may be as follows: First solve the unsteady Reynolds equation without considering external pressurization. With the prescribed $[h_{min}]$ if the computed load carrying capacity exceeds the normal force, hydrostatic lubrication is not needed and one may go right to the next time step. Otherwise activate the procedure described in the previous paragraph.

The discretization of the mathematical problem, the numerical scheme used to integrate in the time domain, and the iteration algorithms will be described in the next report along with the computational results.

4 Summary

Based on the speed ratio and power output requirements of the intended application, a particular type of double-enveloping wormgear is selected. After extensive studies and comparisons, a set of wormgear dimensions and parameters are laid out in such a way that the contact pattern of the meshing tooth surfaces is suitable for implementing hydrostatic lubrication. The kinematic and load sharing properties needed for the lubrication analysis are determined, which include the variation of the clearance between the meshing worm and gear surfaces, their relative velocities, and the normal force acting on a gear tooth during the meshing period.

Based on the kinematic study two fluid film load bearing regions on a gear tooth are located. The oil supply configuration on the tooth surface is designed. Fluid film lubrication of the contact is formulated considering external pressurization as well as hydrodynamic wedge and squeeze actions. The flow in the flow restrictors is analyzed that links the oil supply pressure with the recess pressures, which in turn are linked with the minimum oil film thickness. The lubrication analysis is aimed at obtaining the oil supply pressure needed to separate the worm and gear surfaces by a prescribed minimum oil film thickness. The procedure of solving the mathematical problem is outlined.

References

American Gear Manufactures Association, 1965, "Design of General Industrial Double-Enveloping Wormgears", AGMA Standard 342.02.

Chaiko, L., 1990, "Assessment of Worm Gearing for Helicopter Transmissions", NASA Technical Memorandum 102441, AVSCOM Technical Memorandum 89-C-010.

Dudley, D. W., 1984, Handbook of Practical Gear Design, McGraw-Hill.

Fox, R. W. and McDonald, A. T., 1992, Introduction to Fluid Mechanics, 4th Ed., Wiley.

Liepmann, H. W. and Roshko, A., 1957, Element of Gasdynamics, GALCIT Aeronautical Series.

Moran, M. J. and Shapiro, H. N., 1992, Fundamentals of Engineering Thermodynamics, 2nd Ed., Wiley.

Shen, Y. F. et al., 1983, Meshing of Spatial Mechanisms and the SG-71 Wormgear (in Chinese), Metallurgy Industry Publication Corporation, Beijing.

Sun, D. C., 1991, Mechanics of Lubrication (in Chinese), Friendship Publication Corporation, Beijing.

Sun, D. C. and Yuan, Q., 1994a, "Study of the Kinematic and Dynamic Characteristics of a Wormgear Transmission for Helicopter Applications", NASA Contract Report 195287, Army Research Laboratory Contract Report ARL-CR-78.

Sun, D. C. and Yuan, Q., 1994b, "Study of the Kinematic and Load Sharing Properties of Wormgearing with Non-Symmetric Tooth Profiles", Contract Report submitted to Vehicle Propulsion Directorate, Army Research Laboratory in April.

Table 1 Dimensions and Parameters of the Selected Wormgear

TERM	SYMBOL	VALUE	FORMULA BASED	REFERENCE
speed ratio	i	110		given
normal pressure angle	α_n	20 deg		Dudley, 1984 p. 3.71
center distance	a	880 mm		selected
number of worm threads	N_1	1		selected
number of gear teeth	N_2	110	$N_2 = N_1*i$	
pitch diameter of worm*	d_1	300 mm	$d_1 = a^{0.875}/k_d$ (E) (k_d = 1.7-2.2)	Dudley, 1984 p. 3.70
pitch diameter of gear	d_2	1460 mm	$d_2 = 2*a-d_1$	
axial pitch	p_x	41.6975 mm	$p_x = \pi*d_2/N_2$	Dudley, 1984 Table 3.32
worm lead angle*	γ	2.533 deg	$\tan\gamma = p_x*N_1/\pi/d_1$	Dudley, 1984 Eq. 3.38
normal circular pitch	p_n	41.6568 mm	$p_n = p_x*\cos\gamma$	Dudley, 1984 Table 3.32
axial pressure angle*	α_x	20.018 deg	$\tan\alpha_x = \tan\alpha_n/\cos\gamma$	Dudley, 1984 Eq. 3.40
	$\Delta\alpha$	0.818 deg	$\Delta\alpha = p_x/2/d_2$	Dudley, 1984 p. 3.72
base circle diameter	d_b	519.3182 mm	$d_b = d_2*\sin(\alpha_x+\Delta\alpha)$	Dudley, 1984 Eq. 3.41
module	x_m	13.2727 mm/tooth	$x_m = p_x/\pi$	Dudley, 1984 Table 3.32
number of meshing teeth	N_p	10		selected
half angle of meshing	ψ_a	15.627 deg	$\psi_a = \pi*(N_p-0.45)/N_2$	Shen, 1983 Table 10.1
start angle of meshing	ψ_f	5.209 deg	$\psi_f = \sin^{-1}(d_b/d_2)-\psi_a$	Shen, 1983 Table 10.1
thickness of worm thread	S_1	18.7639 mm	$S_1 = 0.45*p_x$	Dudley, 1984 p. 3.73
thickness of gear tooth	S_2	22.9336 mm	$S_2 = 0.55*p_x$	Dudley, 1984 P. 3.73

whole depth	b_t	20.8284 mm	$b_t = b_k+c$	Dudley, 1984 Table 3.31
working depth	b_k	18.7455 mm	$b_k = 2*b_a$	Dudley, 1984 Table 3.31
addendum	b_a	9.3728 mm	$b_a = k_a*p_n$ ($k_a = 0.225$)	Dudley, 1984 Table 3.31
clearance	c	2.0829 mm	$c = k_c*p_n$ ($k_c = 0.05$)	
throat diameter of worm*	d_{a1}	318.7455 mm	$d_{a1} = d_1+2*b_a$	Shen, 1983 Table 10.1
root diameter of worm*	d_{f1}	277.0888 mm	$d_{f1} = d_{a1}-2*b_t$	Dudley, 1984 Eq. 3.39
throat diameter of gear	d_{a2}	1478.7455 mm	$d_{a2} = d_2+2*b_a$	Dudley, 1984 Table 3.32
root diameter of gear	d_{f2}	1437.0888 mm	$d_{f2} = d_{a2}-2*b_t$	Shen, 1983 Table 10.1
face width of worm	b_1	393 mm	$b_1 = d_2*\sin\psi_a$	Shen, 1983 Table 10.1
face width of gear	b_2	249 mm	$b_2 = (0.9\text{-}1.0)*d_{f1}$	Shen, 1983 Table 10.1
apex angle of generating plane	β	3 deg		selected

* At the center of worm.

Figures

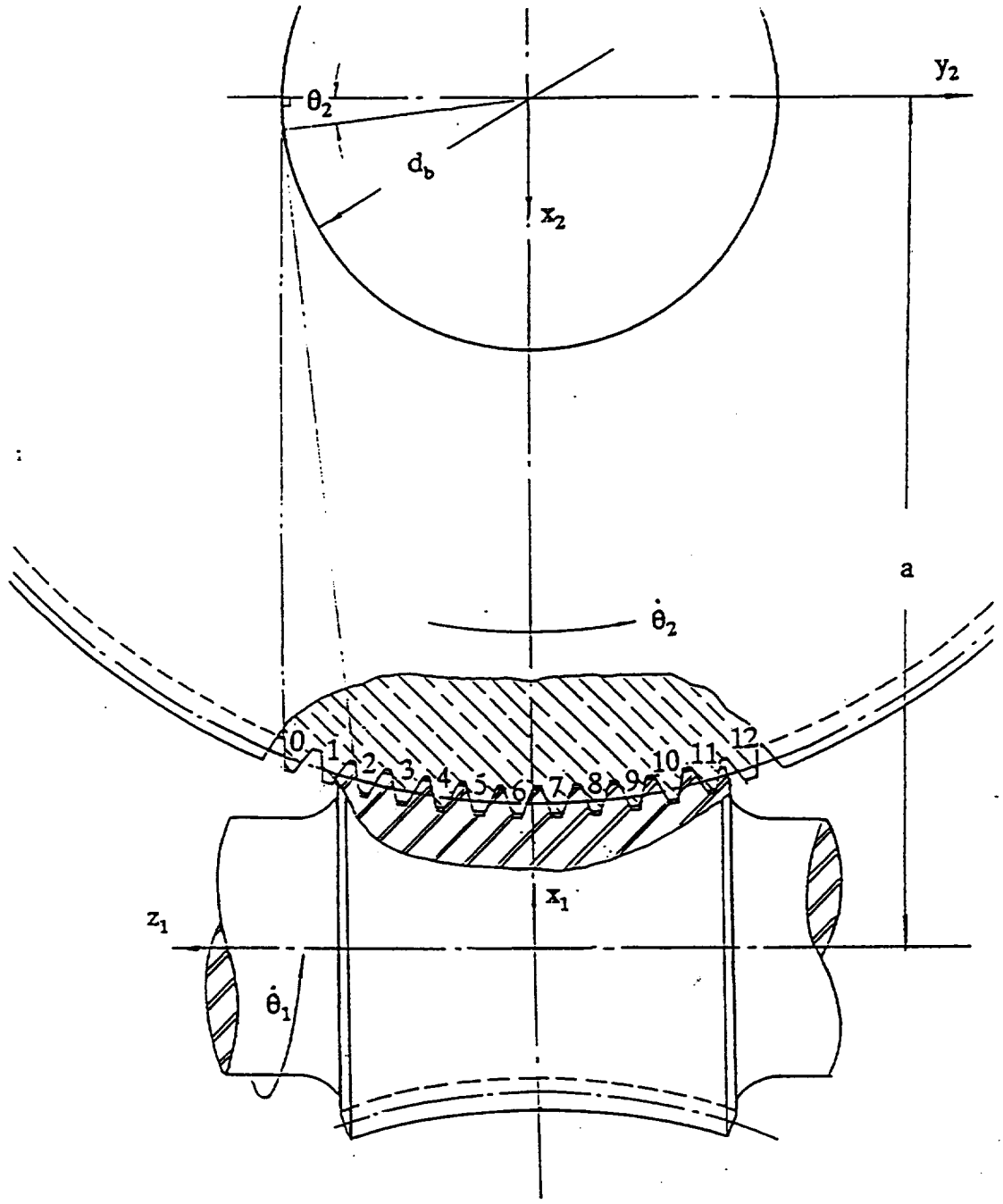

Fig. 1 Wormgear position where gear tooth No. 0 is at $\theta_2 = 0$

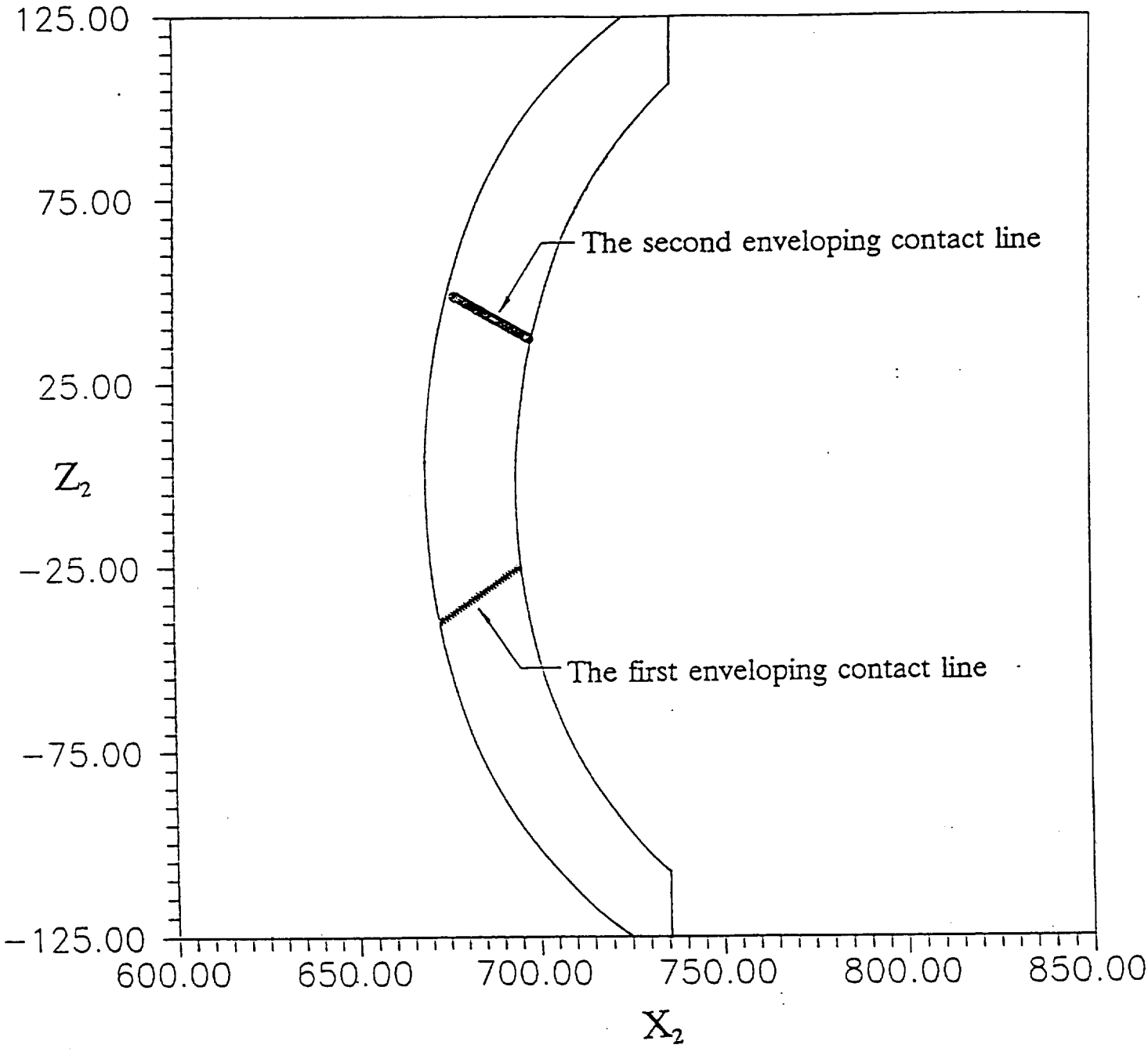

Fig. 2 Contact lines on the gear tooth with α_n = 20 deg, β = 3 deg
(a) tooth position No. 2

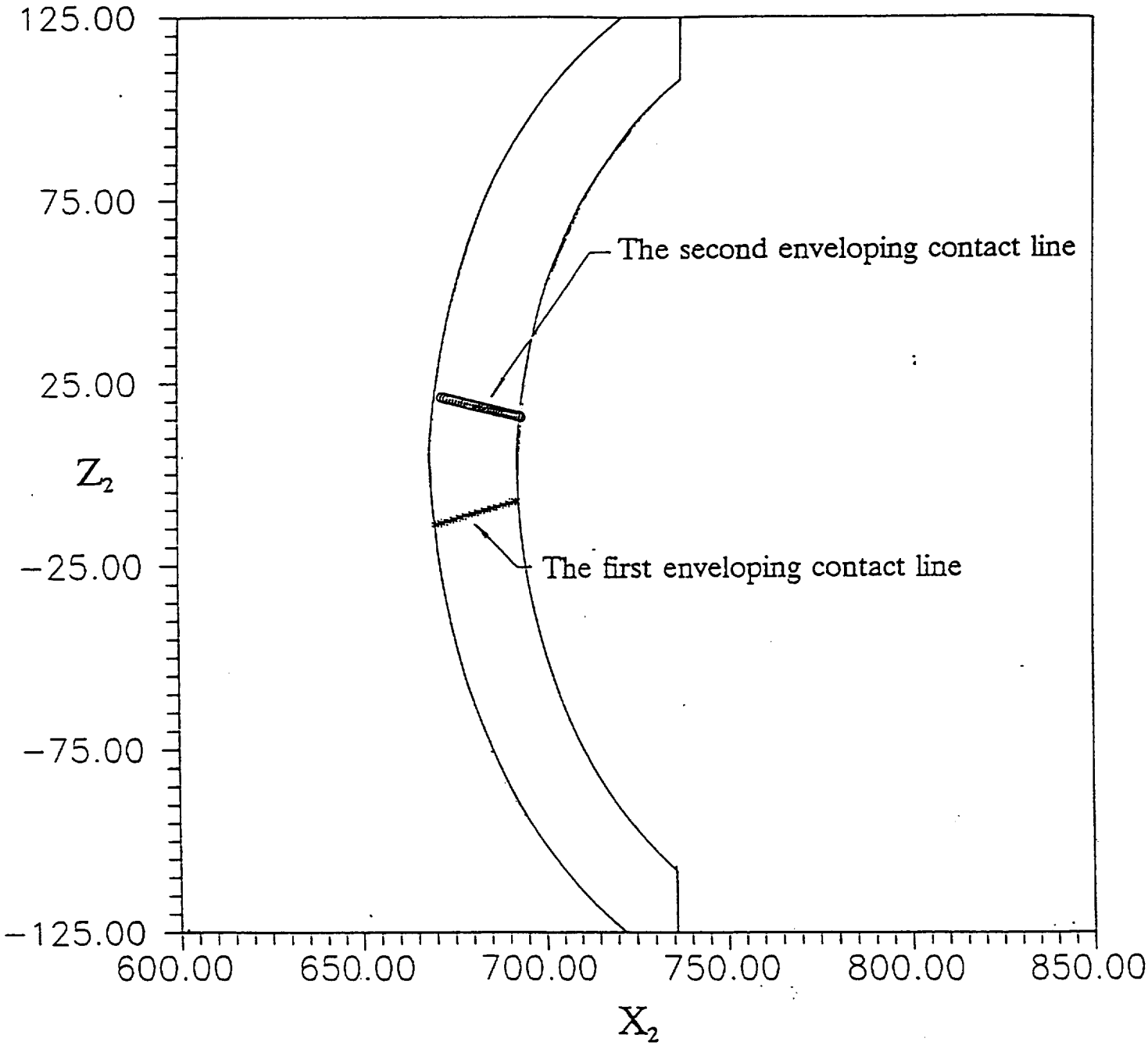

Fig. 2 Contact lines on the gear tooth with α_n = 20 deg, β = 3 deg
(b) tooth position No. 4

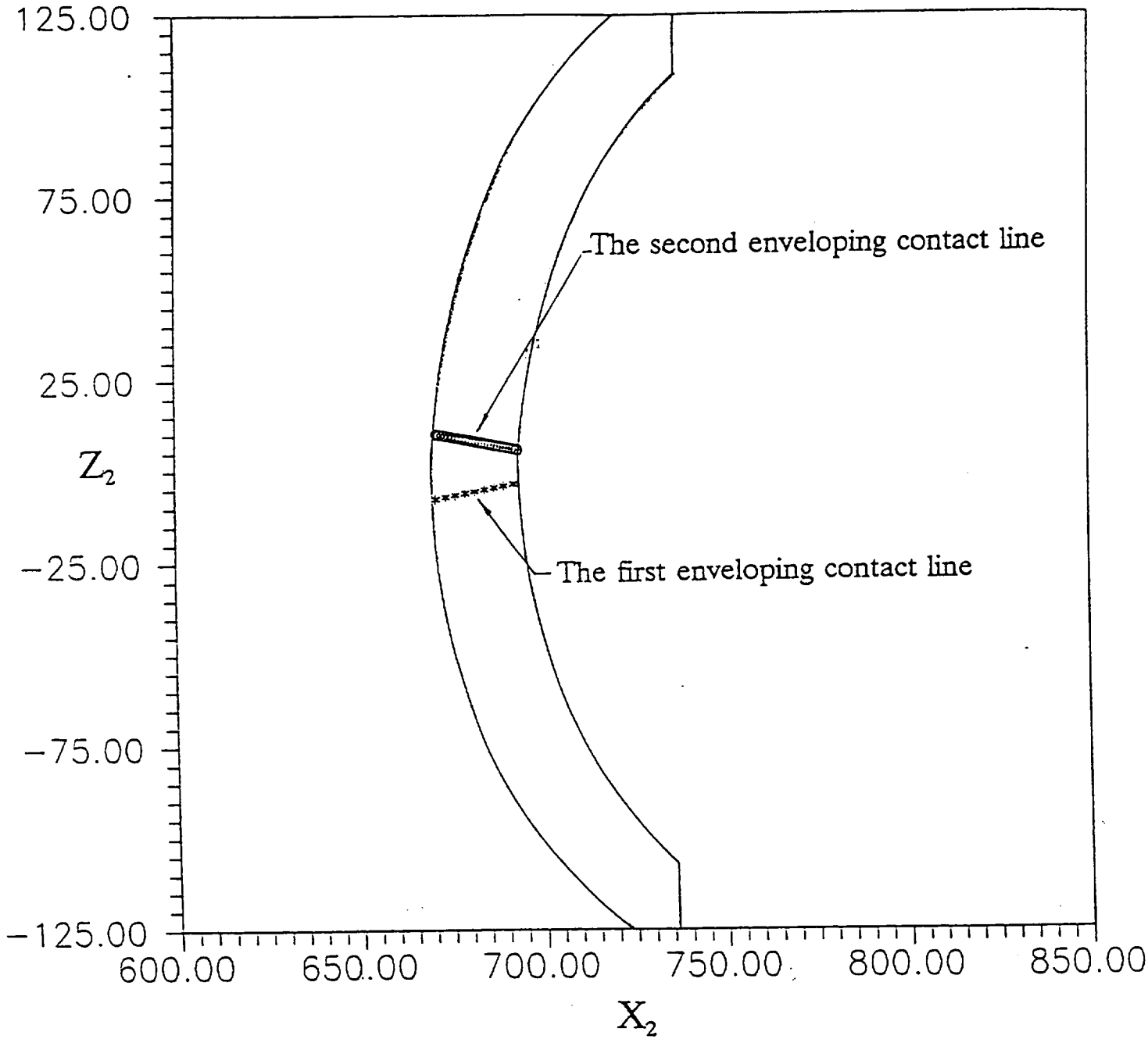

Fig. 2 Contact lines on the gear tooth with α_n = 20 deg, β = 3 deg
(c) tooth position No. 6

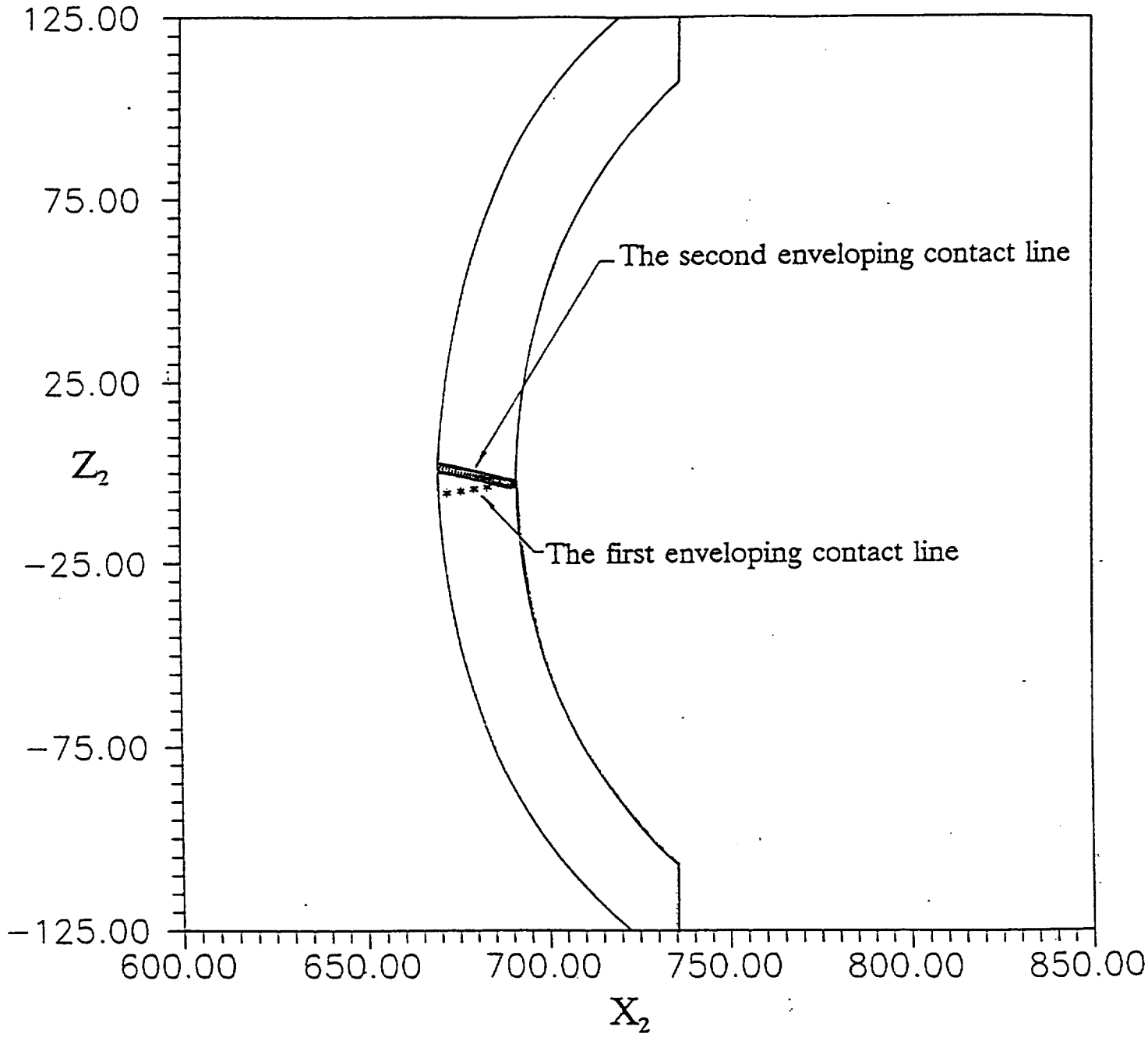

Fig. 2 Contact lines on the gear tooth with α_n = 20 deg, β = 3 deg
(d) tooth position No. 8

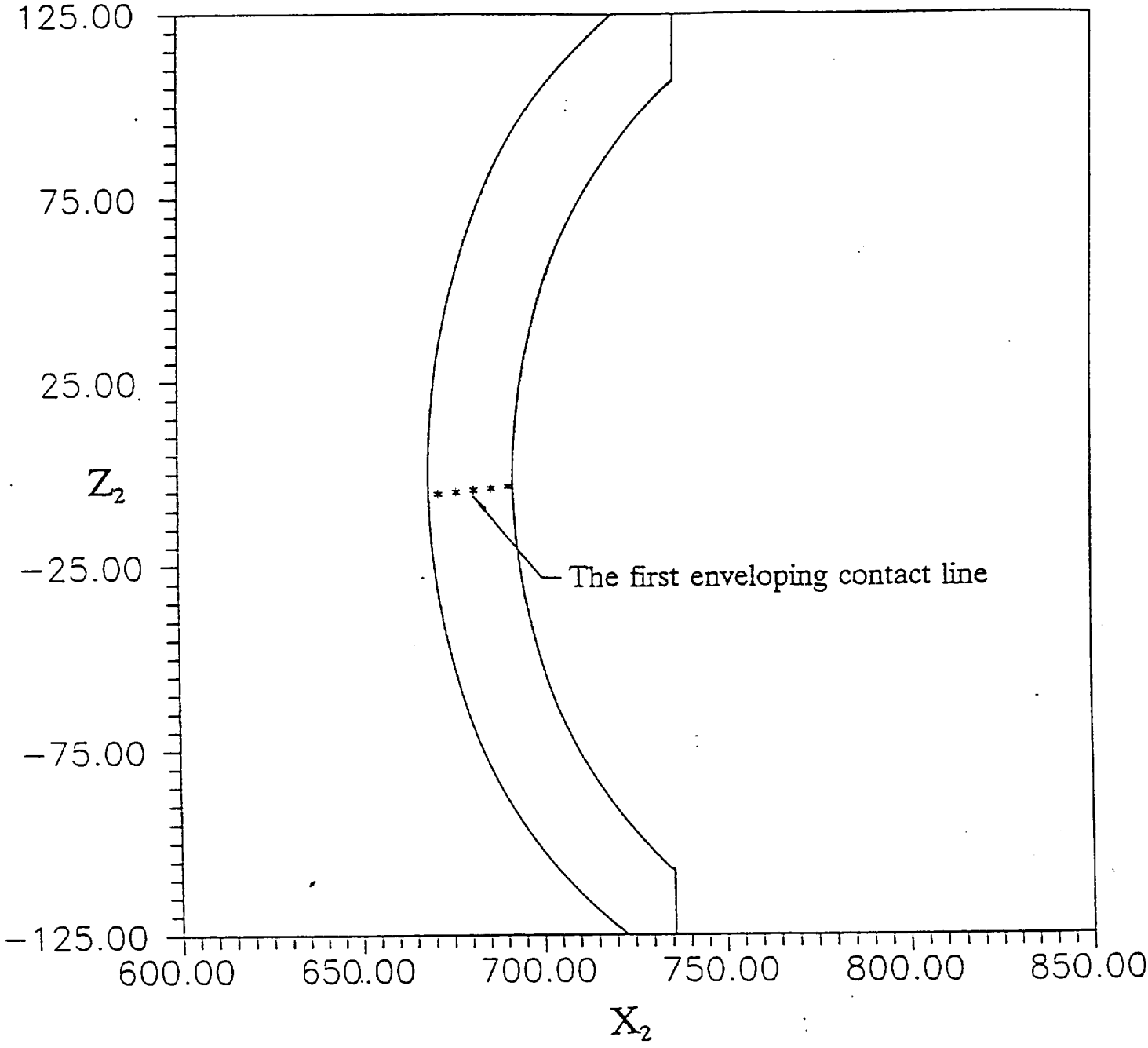

Fig. 2 Contact lines on the gear tooth with α_n = 20 deg, β = 3 deg
(e) tooth position No.10

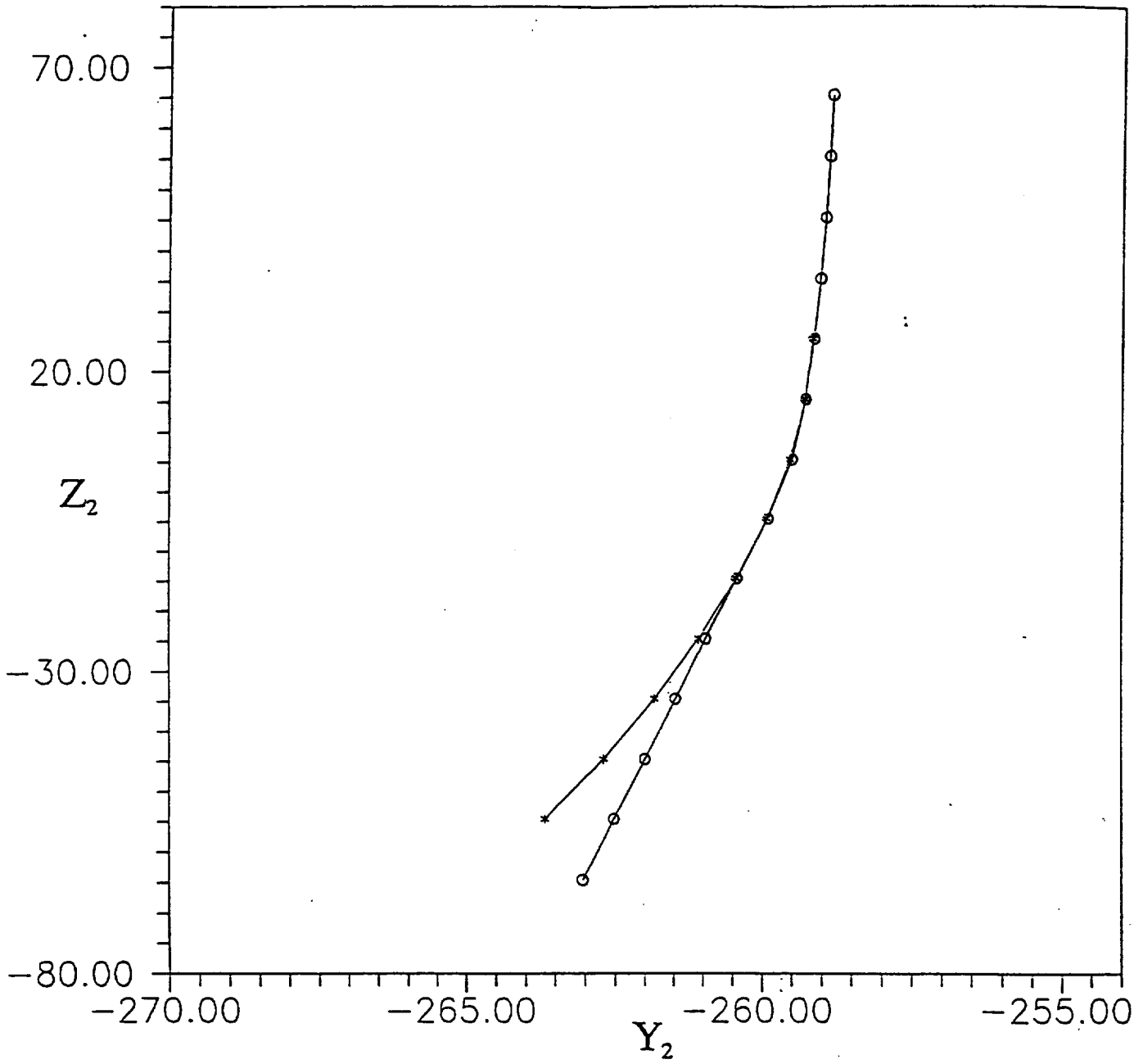

Fig. 3 Variation of clearance on a gear tooth
(a) tooth position No. 2

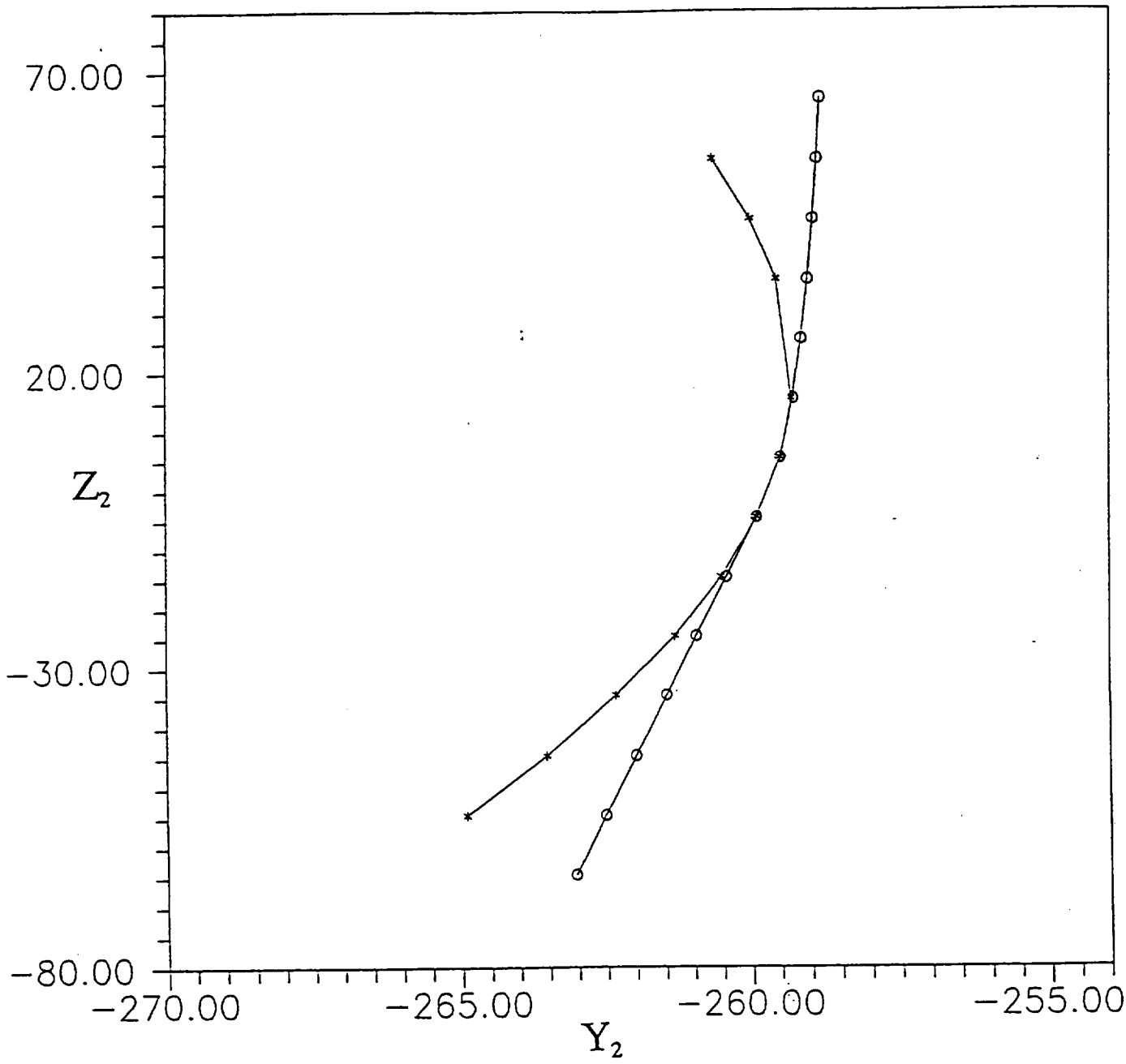

Fig. 3 Variation of clearance on a gear tooth
(b) tooth position No. 4

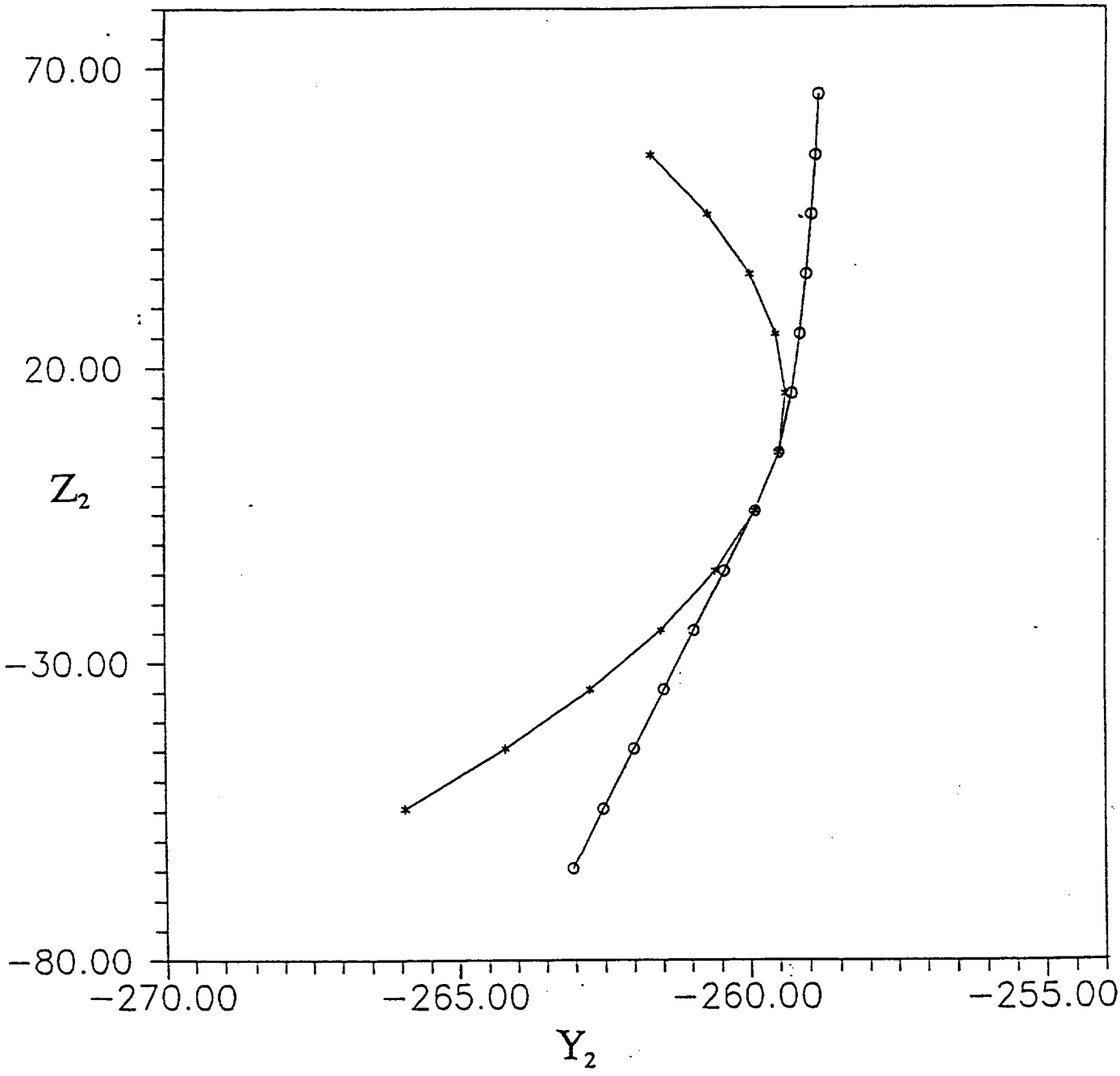

Fig. 3 Variation of clearance on a gear tooth
(c) tooth position No. 6

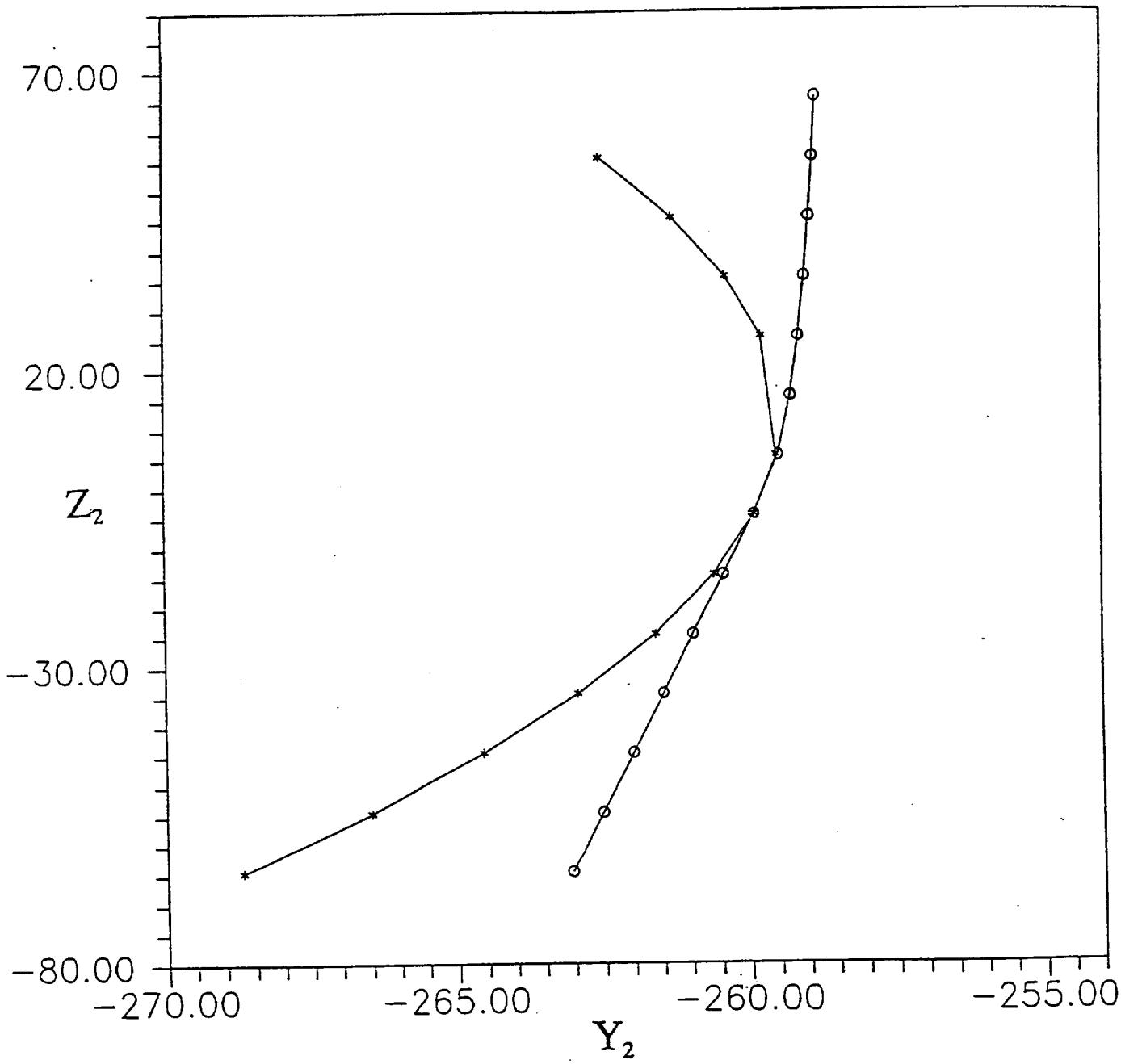

Fig. 3 Variation of clearance on a gear tooth
(d) tooth position No. 8

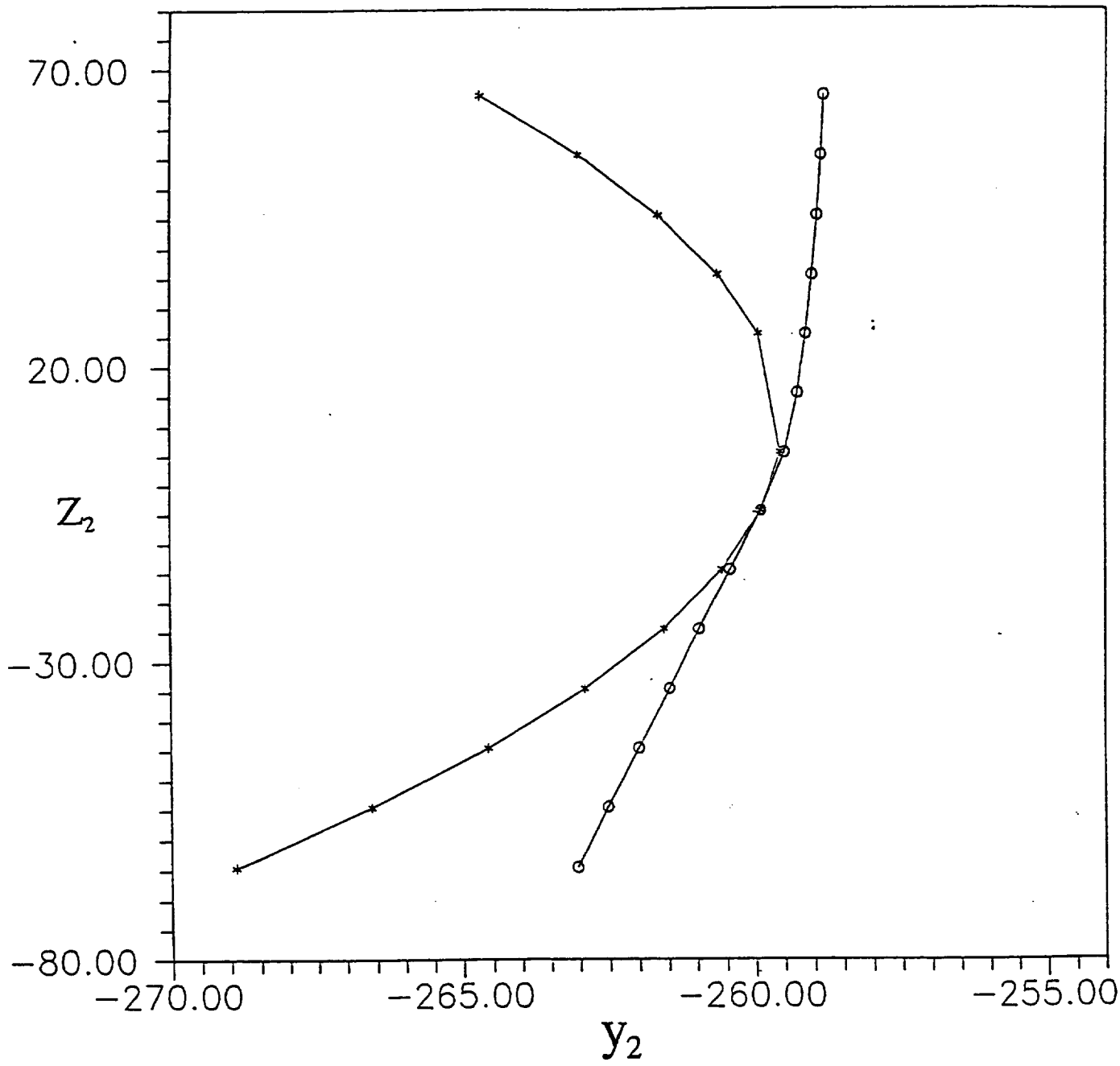

Fig. 3 Variation of clearance on a gear tooth
(e) tooth position No.10

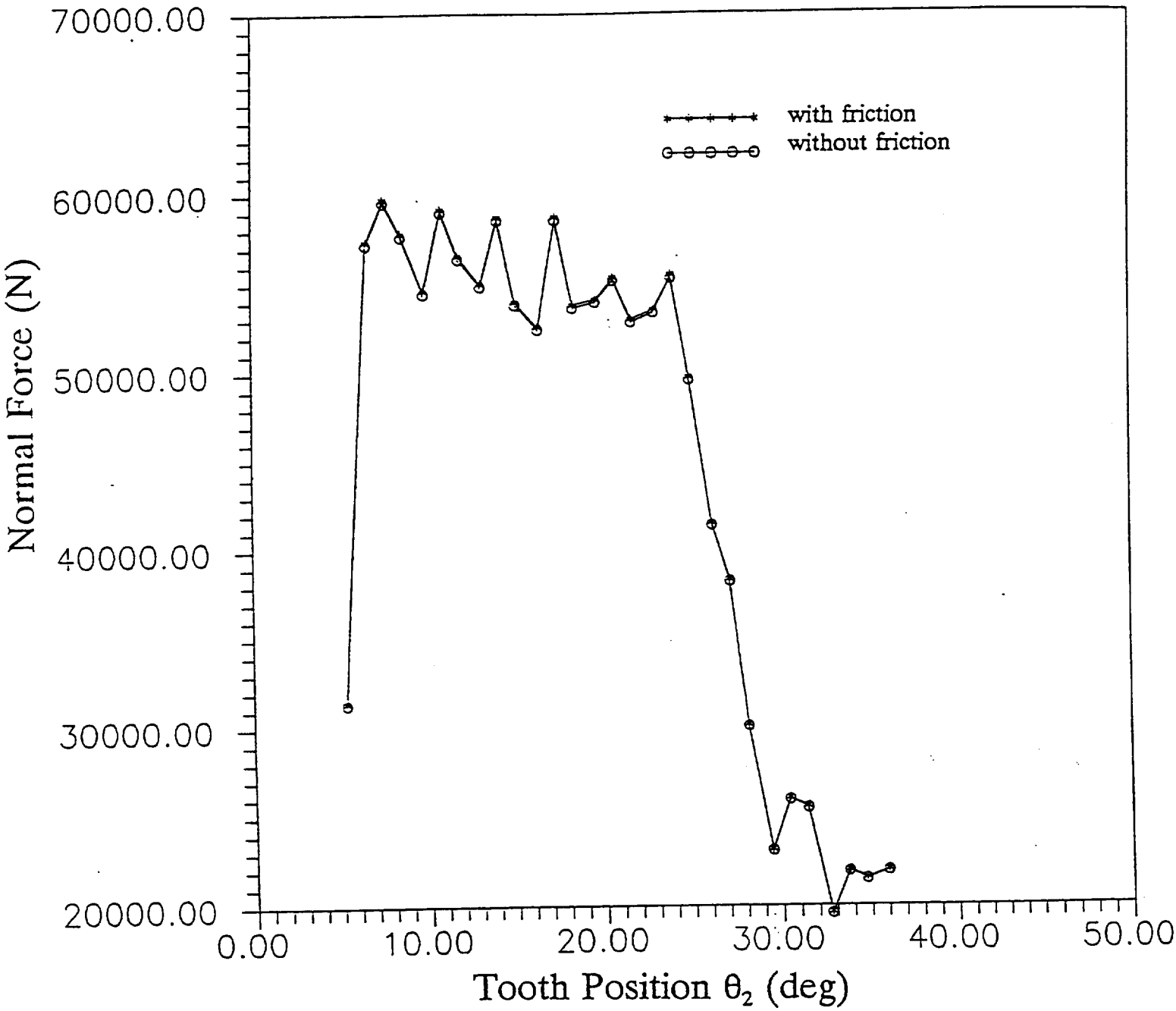

Fig. 4 Variation of normal force on a gear tooth

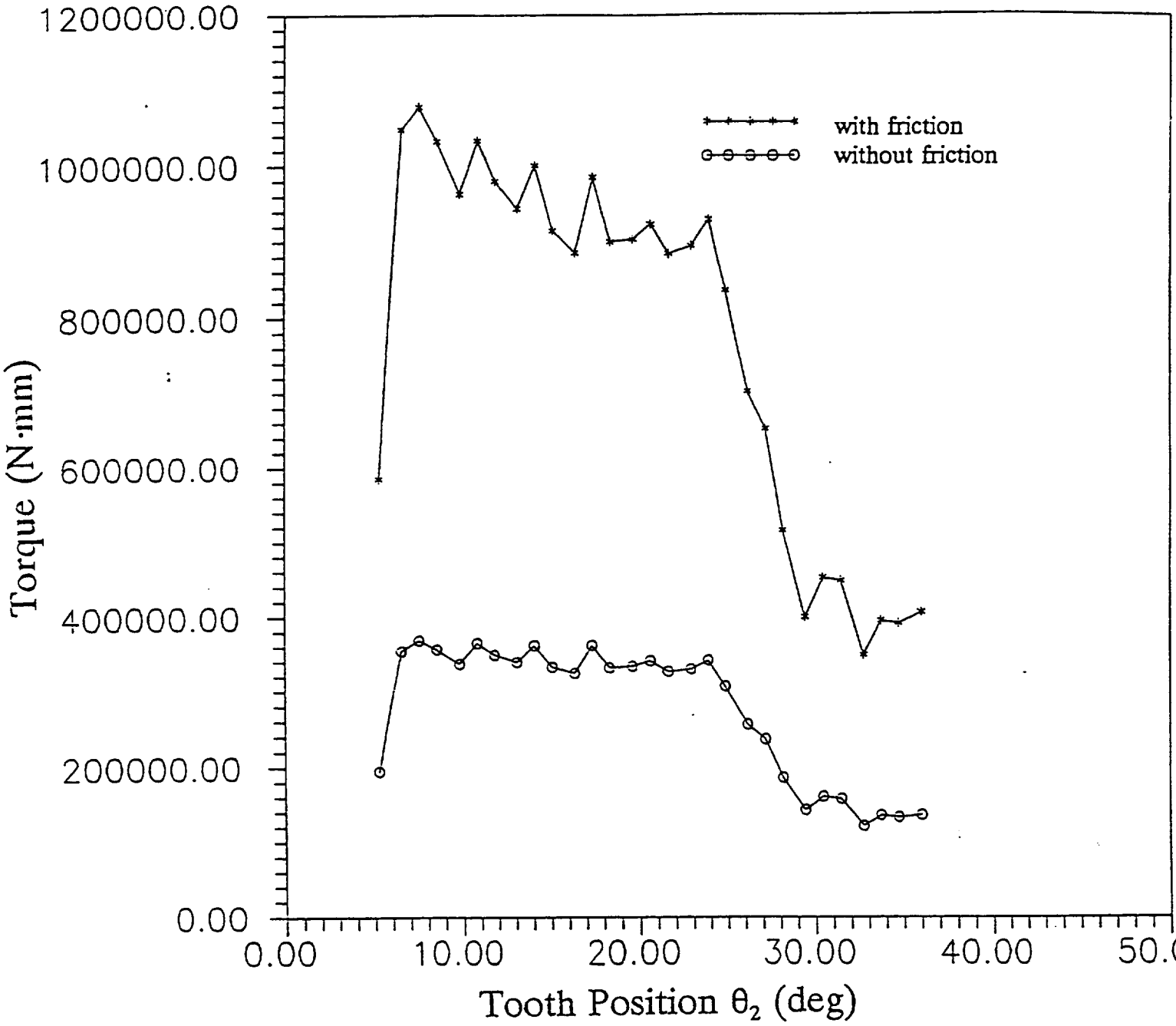

Fig. 5 Variation of torque along the worm coil

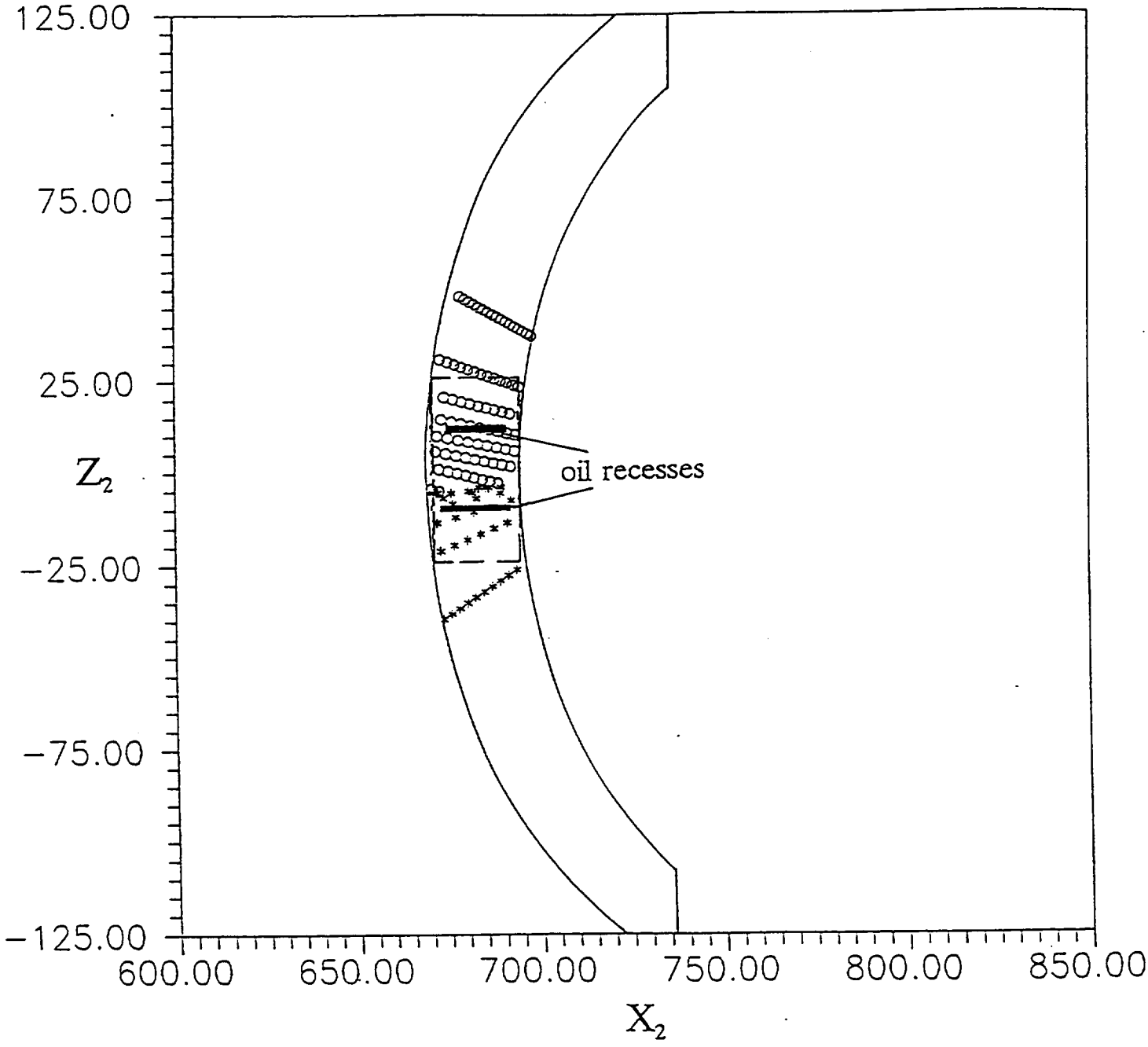

Fig. 6 Lubrication area and location of oil recesses

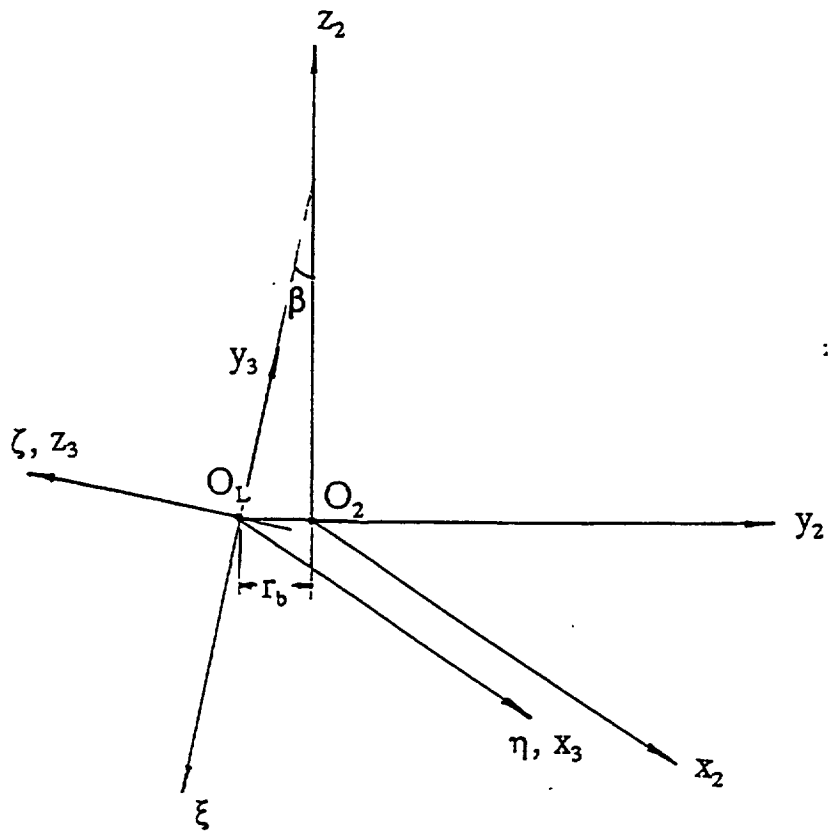

Fig. 7 Coordinate systems for lubrication analysis and clearance calculation

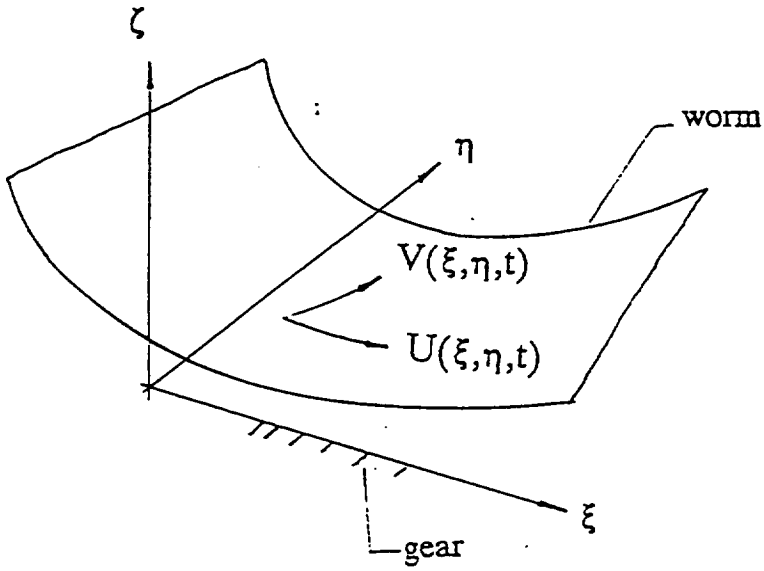

Fig. 8 A schematic diagram of the lubrication model

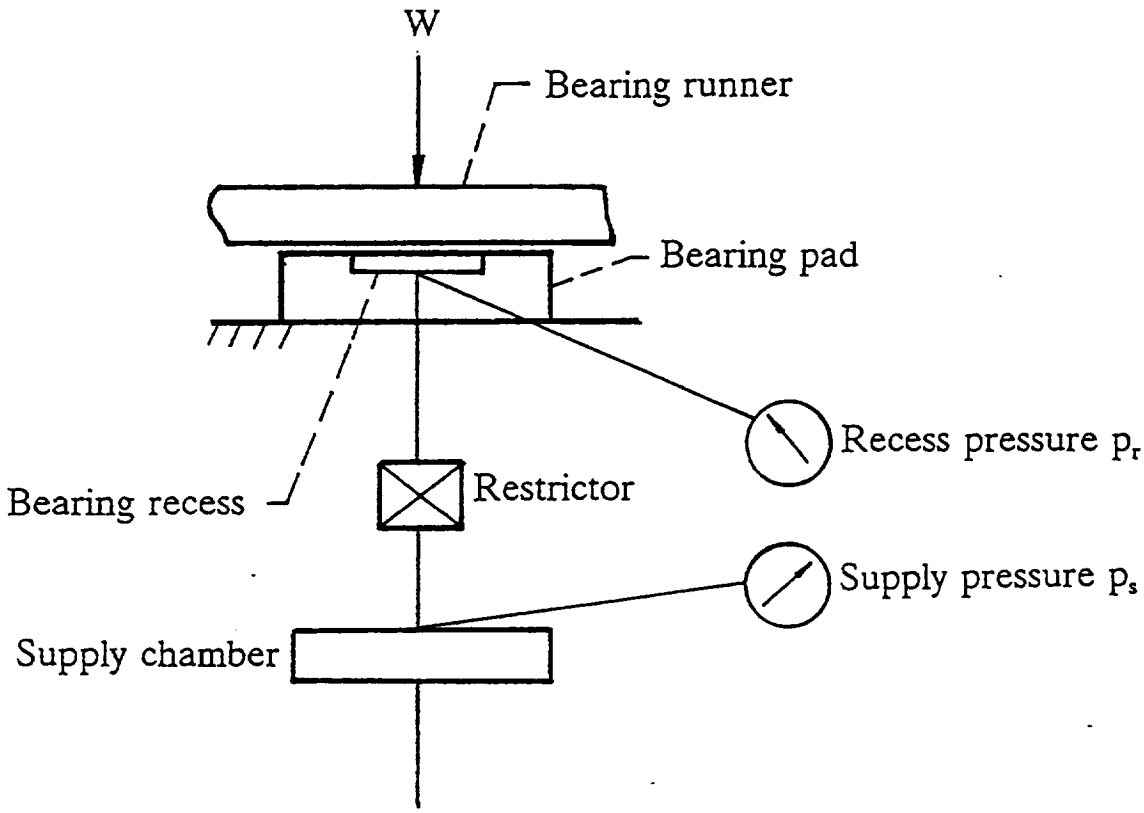

Fig. 9 A schematic diagram of a hydrostatic bearing

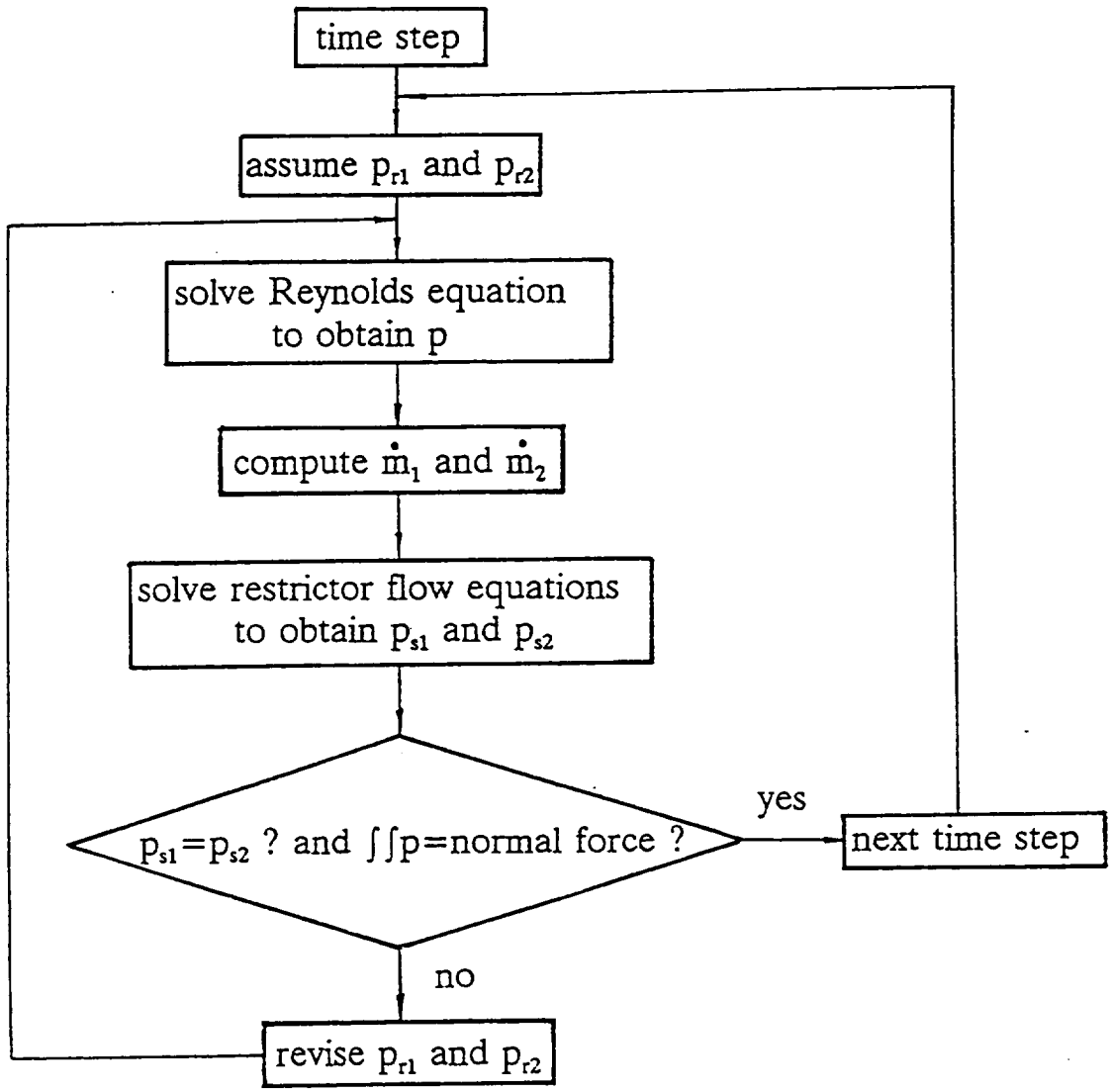

Fig.10 Solution procedure

Appendix 1 Calculation of the Clearance between the Meshing Surfaces

The clearance between the worm and gear surfaces can be obtained numerically. To calculate this quantity, it is convenient to introduce a moving coordinate system $S_3(x_3,y_3,z_3)$, where the (x_3,y_3) plane coincides with the original generating plane; the x_3 axis is in parallel with the x_2 axis; and the origin coincides with the tangent point between the original generating plane and the base circle. The S_3 coordinate system is shown in Fig. 7. The clearance function is then given by:

$$g(\theta,\psi,\theta^*) = z_{W3} - z_{G3} \tag{19}$$

where z_{W3} and z_{G3} may be determined from the following equations:

$$\begin{aligned} A^{(32)} A_\theta^{(21)} F &= 0 \\ A^{(32)} A_\theta^{(21)} D_\psi F &= 0 \\ A^{(32)} A_\theta^{(21)} D_\theta^{(1)} F &= 0 \end{aligned} \tag{20}$$

$$\begin{aligned} A^{(32)} A_{\theta^*}^{(21)} F &= 0 \\ A^{(32)} A_{\theta^*}^{(21)} D_\psi F &= 0 \end{aligned} \tag{21}$$

Since the clearance varies with the rotation of the wormgear, θ^* is used here to denote the current wormgear position. It is not necessary to calculate the clearance beyond the worm and gear tooth domains which are specified in Report 1.

To calculate the clearance one must first locate the corresponding points on the worm and gear surfaces. The procedure to determine the points on the gear surface is as follows: Choose a y_3 value (say, $y_3 = c$) and let θ_2 run through a series of values within the meshing range. The points that satisfy $y_3 = c$ and Eqs. 20 are found by root searching. Then check if these points lie within the gear tooth domain. To locate the points on the worm surface, one must repeat the above procedure for every wormgear position θ^*.

In this case the points must satisfy $y_3 = c$ and Eqs. 21; and these points need to be transformed to S_j to check whether they lie within the worm tooth domain. The two sets of points so obtained are the bases for interpolation to locate the corresponding gear and worm points having the same (x_3,y_3) coordinates. The above calculation steps are repeated for as many y_3 values as needed, in this way all the corresponding points on the meshing surfaces are found.

The coordinate transformation matrices used in the calculations are those between S_2 and S_3,

$$A^{(32)} = \begin{bmatrix} 1 & 0 & 0 & 0 \\ 0 & \sin\beta & \cos\beta & r_b*\sin\beta \\ 0 & -\cos\beta & \sin\beta & -r_b*\cos\beta \\ 0 & 0 & 0 & 1 \end{bmatrix} \tag{22}$$

$$A^{(23)} = \begin{bmatrix} 1 & 0 & 0 & 0 \\ 0 & \sin\beta & -\cos\beta & -r_b \\ 0 & \cos\beta & \sin\beta & 0 \\ 0 & 0 & 0 & 1 \end{bmatrix} \tag{23}$$

and the one from S_3 to S_j for a given wormgear position θ^*:

$$A_{\theta^*}^{(j3)} = A_{\theta^*}^{(j2)} A^{(23)}$$

$$= \begin{bmatrix} -\cos\theta_2^* & \sin\theta_2^*\sin\beta & -\sin\theta_2^*\cos\beta & a-r_b\sin\theta_2^* \\ 0 & -\cos\beta & -\sin\beta & 0 \\ -\sin\theta_2^* & -\cos\theta_2^*\sin\beta & \cos\theta_2^*\cos\beta & r_b\sin\theta_2^* \\ 0 & 0 & 0 & 1 \end{bmatrix} \tag{24}$$

It should be mentioned that a part of the gear surface could be formed not by the enveloping process. Consider the situation where the gear hob has

a face width shorter than the diameter of the base circle. Then, the two ends of the gear tooth (large $\pm z_2$ values) and the central portion of the gear tooth (small $\pm z_2$ values) may be left out by the enveloping process. The former is due to the late engagement, and the latter the early disengagement, between the gear and the hob. Under such a circumstance the portion of the gear surface that is not covered by the enveloping process is described not by Eqs. 20, but instead by the equation of the hob surface.

Another situation may arise where the face width of the worm is shorter than that of the gear hob. Then, even if the entire gear surface is produced by the enveloping process, only a part of it is in contact with the worm during meshing.

In the present study the face width of the worm and that of the gear hob are the same. Using the gear dimensions listed in Table 1, it is found that the gear surface covered by the first and second enveloping contact lines subtends a z_2 range between -195 mm and 150 mm for N_p slightly greater than 13; between -84 mm and 91 mm for $N_p = 12$; and between -37 mm and 48 mm for $N_p = 10$. In contrast, the z_2 range selected for the application of fluid film lubrication is between $\pm$ 25 mm.

Appendix 2 Calculation of the Relative Velocities

Once the corresponding points on the worm and gear surfaces are found, they are transformed to S_j and S_n, respectively. In the stationary coordinate systems the absolute velocities of these points are obtained. Then the velocities of the points on the worm surface are transformed to S_n to form relative velocities with reference to the velocities of the points on the gear surface. Finally, the relative velocities are transformed to S_3 for use in the lubrication analysis.

Because the velocity is a free vector, its transformation takes a 3 x 3 matrix. Suppose the coordinate transformation matrix from S_m to S_k is:

$$A^{(km)} = \begin{bmatrix} a_{11} & a_{12} & a_{13} & a_{14} \\ a_{21} & a_{22} & a_{23} & a_{24} \\ a_{31} & a_{32} & a_{33} & a_{34} \\ 0 & 0 & 0 & 1 \end{bmatrix} \tag{25}$$

Then, the velocity in S_m, $(V_x^{(m)}, V_y^{(m)}, V_z^{(m)})$, is transformed to S_k as:

$$\begin{bmatrix} V_x^{(k)} \\ V_y^{(k)} \\ V_z^{(k)} \end{bmatrix} = \begin{bmatrix} a_{11} & a_{12} & a_{13} \\ a_{21} & a_{22} & a_{23} \\ a_{31} & a_{32} & a_{33} \end{bmatrix} \begin{bmatrix} V_x^{(m)} \\ V_y^{(m)} \\ V_z^{(m)} \end{bmatrix} \tag{26}$$

The velocity of a worm point in S_j is:

$$\vec{V}_W^{(j)} = (V_{WX}^{(j)} , V_{WY}^{(j)} , V_{WZ}^{(j)}) = \vec{\omega}_W \times \vec{r}_W = \begin{vmatrix} \vec{i}^{(j)} & \vec{j}^{(j)} & \vec{k}^{(j)} \\ 0 & 0 & \omega_W \\ x_W^{(j)} & y_W^{(j)} & z_W^{(j)} \end{vmatrix} \tag{27}$$

The velocity of a gear point in S_n is:

$$\vec{V}_G^{(n)} = (V_{GX}^{(n)},\ V_{GY}^{(n)},\ V_{GZ}^{(n)}) = \vec{\omega}_G \times \vec{r}_G = \begin{vmatrix} \vec{i}^{(n)} & \vec{j}^{(n)} & \vec{k}^{(n)} \\ 0 & 0 & \omega_G \\ x_G^{(n)} & y_G^{(n)} & z_G^{(n)} \end{vmatrix} \tag{28}$$

The velocity of a worm point in S_n is:

$$\vec{V}_W^{(n)} = \begin{bmatrix} V_{WX}^{(n)} \\ V_{WY}^{(n)} \\ V_{WZ}^{(n)} \end{bmatrix} = \begin{bmatrix} -1 & 0 & 0 \\ 0 & 0 & -1 \\ 0 & -1 & 0 \end{bmatrix} \begin{bmatrix} V_{WX}^{(j)} \\ V_{WY}^{(j)} \\ V_{WZ}^{(j)} \end{bmatrix} \tag{29}$$

The velocity of a worm point relative to that of a gear point in S_n is:

$$\vec{V}_R^{(n)} = (V_{RX}^{(n)},\ V_{RY}^{(n)},\ V_{RZ}^{(n)}) = (V_{WX}^{(n)} - V_{GX}^{(n)},\ V_{WY}^{(n)} - V_{GY}^{(n)},\ V_{WZ}^{(n)} - V_{GZ}^{(n)}) \tag{30}$$

where the subscript $(\ )_R$ denotes a relative velocity. The relative velocity in S_3 is:

$$\begin{bmatrix} V_{RX}^{(3)} \\ V_{RY}^{(3)} \\ V_{RZ}^{(3)} \end{bmatrix} = \begin{bmatrix} \cos\theta_2^* & \sin\theta_2^* & 0 \\ -\sin\beta\sin\theta_2^* & \sin\beta\cos\theta_2^* & \cos\beta \\ \cos\beta\sin\theta_2^* & -\cos\beta\cos\theta_2^* & \sin\beta \end{bmatrix} \begin{bmatrix} V_{RX}^{(n)} \\ V_{RY}^{(n)} \\ V_{RZ}^{(n)} \end{bmatrix} \tag{31}$$

REPORT DOCUMENTATION PAGE

Form Approved
OMB No. 0704-0188

1. AGENCY USE ONLY (*Leave blank*)	2. REPORT DATE	3. REPORT TYPE AND DATES COVERED
	January 1995	Final Contractor Report

4. TITLE AND SUBTITLE
Wormgear Geometry Adopted for Implementing Hydrostatic Lubrication and Formulation of the Lubrication Problem

5. FUNDING NUMBERS
NAG3–1316
WU–505–62–0J
1L161102AH45

6. AUTHOR(S)
D. C. Sun and Qin Yuan

7. PERFORMING ORGANIZATION NAME(S) AND ADDRESS(ES)
State University of New York
Department of Mechanical Engineering
Binghamton, New York 13902–6000

8. PERFORMING ORGANIZATION REPORT NUMBER
E–9345

9. SPONSORING/MONITORING AGENCY NAME(S) AND ADDRESS(ES)
National Aeronautics and Space Administration
Washington, D.C. 20546–0001
and
U.S.Army Research Laboratory
Adelphi, Maryland 20783–1145

10. SPONSORING/MONITORING AGENCY REPORT NUMBER
NASA CR–195416
ARL–CR–219

11. SUPPLEMENTARY NOTES
Project manager, David E. Brewe, Vehicle Propulsion Directorate, U.S. Army Research Laboratory, NASA Lewis Research Center, organization code 5140, (216) 433–6067.

12a. DISTRIBUTION/AVAILABILITY STATEMENT
Unclassified - Unlimited
Subject Category 37

This publication is available from the NASA Center for Aerospace Information, (301) 621–0390.

12b. DISTRIBUTION CODE

13. ABSTRACT (*Maximum 200 words*)

The geometrical parameters for a wormgear intended to be used as the transmission in advanced helicopters are finalized. The resulting contact pattern of the meshing tooth surfaces is suitable for the implementation of hydrostatic lubrication. Fluid film lubrication of the contact is formulated considering external pressurization as well as hydrodynamic wedge and squeeze actions. The lubrication analysis is aimed at obtaining the oil supply pressure needed to separate the worm and gear surfaces by a prescribed minimum film thickness. The procedure of solving the mathematical problem is outlined.

14. SUBJECT TERMS	15. NUMBER OF PAGES
Wormgear; Gears; Transmission; Lubrication; Dynamic; Helicopter; Gearing; Hydrostatic	48
	16. PRICE CODE A03

17. SECURITY CLASSIFICATION OF REPORT	18. SECURITY CLASSIFICATION OF THIS PAGE	19. SECURITY CLASSIFICATION OF ABSTRACT	20. LIMITATION OF ABSTRACT
Unclassified	Unclassified		